PHYSICAL REVIEW B, VOLUME 63, 064501

Critical transverse forces in weakly pinned driven vortex systems

Hans Fangohr,[1,2] Peter A. J. de Groot,[2] and Simon J. Cox[1]
[1]*Department of Electronics and Computer Science, University of Southampton, Southampton, SO17 1BJ, United Kingdom*
[2]*Department of Physics and Astronomy, University of Southampton, Southampton, SO17 1BJ, United Kingdom*
(Received 14 July 2000; published 10 January 2001)

We present simulation results of the moving Bragg glass régime of a driven two-dimensional vortex system in the presence of a smoothly varying weak pinning potential. We study the critical transverse force and (i) demonstrate that it can be an order of magnitude larger than previous estimates and (ii) show that it is still observable when the system is driven along low higher-order lattice vectors. We confirm theoretical predictions that the critical transverse force is the order parameter of the so-called moving glass phase, and provide data to support experimentalists verifying the existence of a critical transverse force.

DOI: 10.1103/PhysRevB.63.064501 PACS number(s): 74.60.Ge

I. INTRODUCTION

The vortex state is dominated by the competition of ordering and disordering interactions. Vortex-vortex repulsion tends to order the system whereas thermal fluctuations and pinning from material imperfections introduce disorder into the vortex lattice. Recently, interest has developed in the nature of the nonequilibrium states and dynamical phases in the presence of a Lorentz force driving the system. There is evidence from experiments,[1] simulations,[2–6] and theory[2,7–9] that for small driving forces the vortex system is disordered and shows turbulent plastic flow, and that for larger driving forces the system orders and shows elastic flow. For the ordered system Koshelev and Vinokur[2] proposed that the vortices may form a moving hexagonal crystal. Subsequently, Giamarchi and Le Doussal[7,8] predicted that this highly driven phase may be a topologically ordered moving glass (the moving Bragg glass) in which vortices move in elastically coupled static channels like beads on a string. It was also suggested[8–10] that the motion of vortices in different channels may be decoupled (the moving transverse glass) and thus shows smectic order. In computer simulations[4–6] and in experiments[11] both the moving transverse glass (MTG) with decoupled channels and the moving Bragg glass (MBG) with coupled channels have been observed.

A remarkable property of the moving glass (with either coupled or decoupled channels) is that, in the presence of random pinning and once the static channels are established, the application of a small force transverse to the direction of motion does not result in transverse motion.[7,8] Only if a critical transverse force has been exceeded, is the system transversely depinned. Computer simulations have demonstrated the existence of such a critical transverse force for random pinning,[4,5,12,13] and for periodic pinning.[14]

In this work we use a more realistic representation of high purity single crystals used in fundamental studies of vortex dynamics; we investigate régimes with a high density of vortices with long-range logarithmic vortex-vortex interaction potentials (as in Ref. 12) and we employ a weak smoothly varying pinning potential rather than many strong pointlike pins.[4,5,12,13] We find and explain a magnitude of the critical transverse force of the order of 10% of the static depinning force in the régime investigated in contrast to previous works[4,5,13] which report it to be $\approx 1\%$. We report on results for the critical transverse force in the presence of weak pinning which (i) verify the theory of Giamarchi and Le Doussal[7] and (ii) provide numerical data which may be compared directly with current experimental efforts to demonstrate the existence of the critical transverse force.

II. THE SIMULATION

We model the vortex motion of a two-dimensional system with overdamped Langevin dynamics. The total force acting on vortex i is given by $\mathbf{F}_i = -\eta \mathbf{v}_i + \mathbf{F}^{\mathrm{L}} + \mathbf{F}_i^{\mathrm{vv}} + \mathbf{F}_i^{\mathrm{vp}} + \mathbf{F}_i^{\mathrm{therm}} = \mathbf{0}$, where η is the viscosity coefficient, $\mathbf{v}_i$ the velocity, $\mathbf{F}^{\mathrm{L}}$ the Lorentz force, $\mathbf{F}_i^{\mathrm{vv}}$ the vortex-vortex interaction, $\mathbf{F}_i^{\mathrm{vp}}$ the vortex-pinning interaction, and $\mathbf{F}_i^{\mathrm{therm}}$ a stochastic noise term to model temperature. The vortex-vortex interaction force appropriate for rigid vortices in thin films and pancakes in decoupled layers of layered materials is[15] $\mathbf{F}_i^{\mathrm{vv}} = (\Phi_0^2 s)(2\pi\mu_0\lambda^2)^{-1}\Sigma_{j\neq i}(\mathbf{r}_i - \mathbf{r}_j)(|\mathbf{r}_i - \mathbf{r}_j|)^{-2}$. Φ_0 is the magnetic flux quantum, μ_0 the vacuum permeability, and s the length of the vortex. We employ periodic boundary conditions and cut off the logarithmic vortex-vortex repulsion potential at half the system size. It is important to reduce the vortex-vortex interaction near the cut-off distance smoothly to zero.[16] We investigate systems with a magnetic induction of $B = 1$ T and a penetration depth of $\lambda = 1400$ Å which yields a vortex density of $\approx 10/\lambda^2$. The random pinning potential as shown in Fig. 1 varies smoothly on a length scale of $\lambda/25$ which is of the order of magnitude of the coherence length ξ. The root-mean-square value of the corresponding pinning forces is denoted by $F_{\mathrm{rms}}^{\mathrm{vp}}$. System sizes from 100 to 3000 vortices have been investigated. Forces are expressed in units of the force, f_0, that two vortices separated by λ experience.

Initially, we anneal the vortex system in the presence of random pinning from a molten state to zero temperature. Then a driving force is applied which is increased every $4 \cdot 10^4$ time steps. With increasing driving force we find a pinned system, turbulent plastic flow, and finally the MBG. For sufficiently strong pinning there is an intermediate régime between turbulent plastic flow and the MBG in which the vortex motion in different channels is decoupled.[17] We

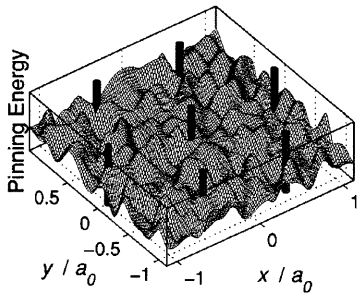

FIG. 1. A sample pinning potential. Distances in x and y directions are given in multiples of the vortex lattice spacing, a_0. The seven black cylinders indicate vortex lines separated by a_0 to demonstrate the length scale.

find a critical transverse force for both the MBG and the MTG, and here we report on the small pinning strengths which do not allow smectic states with decoupled motion of channels of vortices. To find the critical transverse force we start with a MBG driven by a constant force F_x^{L} in the x direction and slowly increase the transverse force F_y^{L} in the y direction, until the system starts moving transversely. The lower ends of the bars shown in Figs. 2 to 5 represent the largest probed transverse force which did not yield any transverse motion, and the upper ends of the bars show the smallest transverse force that could depin the system transversally.

III. RESULTS

Figure 2 shows that there is a decrease in the ratio of the critical transverse force F_y^c to the static depinning force F_x^c for system sizes below 1000 vortices. However, for larger systems this ratio remains constant, showing that the observed F_y^c is not a finite-size effect. We have increased the cut-off with the system size to ensure that effects due to the long-range interactions between the additional particles in the simulation are taken into account, which contrasts to a similar finite-size study[13] where the cut-off for the vortex-vortex interaction was kept constant and the results were reported to be independent of the system size.

Previous estimates[4,5,13] for the ratio F_y^c/F_x^c give a value ≈ 0.01. We find $F_y^c/F_x^c \approx 0.1$ and identify two reasons for this

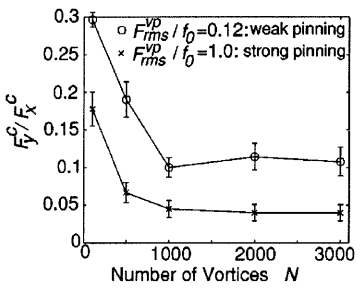

FIG. 2. The ratio of the critical transverse force F_y^c to the static depinning force F_x^c for various numbers of vortices, N. The lower curve is for strong pinning with $F_{\mathrm{rms}}^{\mathrm{vp}}/f_0 = 1.0$ and the upper curve is for weak pinning with $F_{\mathrm{rms}}^{\mathrm{vp}}/f_0 = 0.12$.

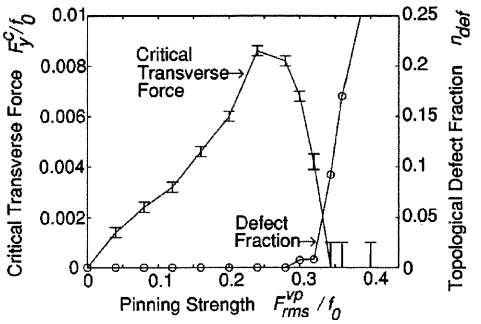

FIG. 3. Critical transverse force and topological defect fraction n_{def} as a function of pinning strength. The critical transverse force reduces to zero where the system changes from elastic flow to turbulent plastic flow and the number of topological defects increases rapidly.

order of magnitude discrepancy. Firstly, we study the weak pinning régime in which the hexagonal structure of the *static* vortex system (i.e., without an applied driving force) is not completely destroyed due to the vortex pinning, whereas previous studies focused on the strongly pinned régime in which the *static* system is strongly disordered. Both systems — with weak and strong pinning — move elastically and show topological order under the influence of the driving force in the x direction. The critical force required to depin the static system, F_x^c, is greater for the strongly pinned system which shows disorder, because a disordered system can adopt better to the pinning potential. However, the force required to depin the moving system transversely, the critical transverse force F_y^c, depends less strongly on the pinning strength because the elastically moving system is topologically ordered for either pinning strength. Thus, the ratio F_y^c/F_x^c is higher for weak pinning. We demonstrate this in Fig. 2 where we show that the change from strong to weak pinning increases the ratio F_y^c/F_x^c by a factor 2 to 3. Secondly, the pinning potentials employed in Refs. 4, 5, and 13 consist of (strong) point-like randomly distributed pins, which we find increase the static depinning force F_x^c by another factor of 2 to 3 compared with using a smoothly varying pinning potential (Fig. 1). We would thus get to the same order of magnitude for the ratio F_y^c/F_x^c as Refs. 4, 5, and 13 if we used the simulation scenario they employed. We find that for different random pinning configurations the F_y^c can vary up to a factor of 2 in the weak pinning limit.

Figure 3 shows the variation of F_y^c as a function of the pinning strength for systems driven with a constant driving force $F_x^{\mathrm{L}} = 0.3 f_0$ in the x direction. The absence of transverse barriers for zero pinning strength shows that it is not the periodic boundary conditions which result in a critical transverse force. With increasing pinning strength F_y^c increases linearly until it starts to decay for pinning strengths of $F_{\mathrm{rms}}^{\mathrm{vp}} \approx 0.25 f_0$ and reaches zero at $F_{\mathrm{rms}}^{\mathrm{vp}} \approx 0.35 f_0$. The decay of the F_y^c is caused by the strength of the pinning producing turbulent plastic flow of the vortices: in this region the MBG breaks down. This is demonstrated by the second curve in Fig. 3 which shows that the fraction of vortices that are to-

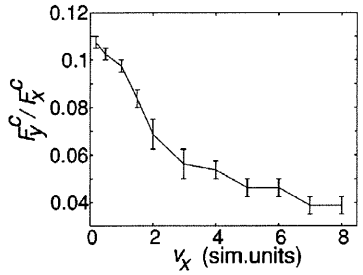

FIG. 4. Critical transverse force F_y^c normalized by the static depinning force F_x^c for various longitudinal velocities v_x in the moving Bragg glass régime.

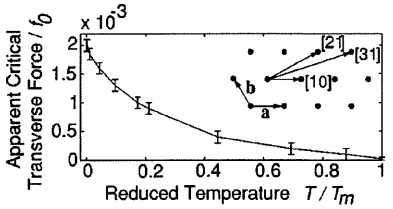

FIG. 5. Apparent critical transverse force as a function of reduced temperature T/T_m. Inset: directions of the driving force probed for the existence of static channels and critical transverse forces. The lattice vectors used for labeling the directions are shown as (a) and (b).

pological defects, n_{def}, increases rapidly for pinning strengths greater than $0.325 f_0$. We define a topological defect to be one which does not have six nearest neighbors in the periodic Delaunay triangulation of the vortex positions. The slight increase of n_{def} for pinning strengths $0.3 f_0$ and $0.325 f_0$ is due to strong temporary deformations of the MBG such that pairs of topological defects appear next to each other and disappear after a few time steps. This indicates the weakness of the MBG but not its breakdown (because the system shows elastic motion). In contrast, the transition to turbulent plastic flow is accompanied by a proliferation of topological defects. This confirms theoretical expectations[8] that the critical transverse force, F_y^c, is the order parameter for the moving glass, which, in the weak pinning régime, is represented by the MBG. The data shown in Fig. 3 are obtained for a system of 576 vortices. For larger systems we get qualitatively the same curves, with a slightly reduced height of F_y^c.

Le Doussal and Giamarchi[8] suggested a dependence of the critical transverse F_y^c as a function of the longitudinal velocity, v_x, which predicts a decay of the F_y^c for large v_x and has not previously been investigated numerically. For an isotropic system one expects that the critical "transverse" force F_y^c for a static system is the same as the critical force (acting in any direction) that is required to depin the system. Our computations confirm that in particular $F_y^c = F_x^c$ for a static system. However, as soon as the system of vortices is depinned and moves elastically in the x direction, the transverse critical force reduces to much smaller values because the system is not sticking to the pinning potential, but depinned in the x direction. Figure 4 shows results of our simulations using a pinning strength of $F_{\mathrm{rms}}^{\mathrm{vp}} = 0.12 f_0$ and a system size of 1200 vortices. We could not resolve the smallest velocities because these are computationally expensive, and we have omitted the data point at $v_x = 0$. The curve starts for small v_x with a F_y^c of $\approx 10\%$ of the static depinning force F_x^c. With increasing v_x the F_y^c decreases quickly up to velocities of ≈ 2 simulation units and then less strongly for larger velocities. Our findings are compatible with the prediction that the critical transverse force decays for higher velocities as additional dynamic disorder weakens the transverse barriers.[8]

The velocities given here in simulation units are directly comparable to Ref. 17, where 0.1 represents a low velocity for the system, and 10 is large. In these units the transition from plastic to elastic flow happens around a velocity of 7 simulation units with a pinning strength of $F_{\mathrm{rms}}^{\mathrm{vp}} = 1.0 f_0$. Our work suggests therefore that small driving forces are most appropriate for experimental verification of the critical transverse force.

It is worth noting that using a system size of less than 1000 vortices (Fig. 2) gives qualitatively different results; for such small systems the F_y^c in Fig. 4 remains constant above a small velocity of ≈ 0.3 simulation units, which is a finite-size effect.

We report on the existence of the critical transverse force in higher commensuration directions. The data shown in Figs. 2 to 6 are obtained with a driving force acting in the [10] (or equivalent symmetry) directions of the Bragg-Glass lattice (see inset Fig. 5). The theory of Giamarchi and Le Doussal[7] predicts that the system should see static disorder when moving in any commensurate direction. It is then expected that the channels and transverse pinning should exist for low commensuration vectors and become unstable at higher ones due to the relatively increasing dynamic disorder.[7] To test these ideas, we have applied a driving force to a hexagonal lattice in the [21] and [31] direction. For the [21] direction we observe that static channels characteristic of the MBG establish and that there are transverse barriers to a transverse force which is subsequently applied. In contrast, we have found that for the [31] directions static Bragg channels do not develop. We presume them to be unstable (at these velocities), and consequently, no critical transverse force has been found for the [31] direction.

For finite temperatures it is predicted that there is no true critical transverse force but all transverse drives result in a small response in the transverse motion of the system.[8] However, for an apparent critical transverse force the system is expected to start moving transversely much quicker. Data on the apparent critical transverse force in Fig. 5 shows that it decays with increasing temperature and vanishes at the melting temperature of the system. The depinning force of the static system, F_x^c, decays similarly with increasing temperature, such that $F_x^c / F_y^c \approx \mathrm{const}$.

To assist in the experimental demonstration of the existence of the critical transverse force we provide in Fig. 6 data on the differential transverse resistance $R_y^{\mathrm{diff}} = \mathrm{d}v_y / \mathrm{d}F_y^{\mathrm{L}}$ normalized by the longitudinal resistance $R_x = v_x / F_x^{\mathrm{L}}$, which

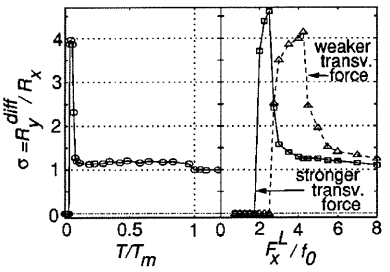

FIG. 6. Differential resistance in transverse direction normalized by resistance in longitudinal direction as a function of reduced temperature (left) and of strength of the longitudinal driving force (right). See text for details.

can both be measured experimentally. We use central differences to approximate the differential transverse resistance

$$R_y^{\mathrm{diff}} = \frac{\mathrm{d}v_y}{\mathrm{d}F_y^{\mathrm{L}}} \approx \frac{v_y(F_y^{\mathrm{L}}+\Delta) - v_y(F_y^{\mathrm{L}}-\Delta)}{2\Delta},$$

where Δ is a small change in force. We compute $\sigma = R_y^{\mathrm{diff}}/R_x$, which is a function of temperature, T, and both components, F_x^{L} and F_y^{L}, of the driving force: $\sigma = \sigma(T, F_x^{\mathrm{L}}, F_y^{\mathrm{L}})$. We choose a small transverse force, F_y^{L}, and keep it constant for each curve in Fig. 6. In the left plot we show $\sigma(T, F_x^{\mathrm{L}} = 1 f_0, F_y^{\mathrm{L}} = 0.00225 f_0)$, i.e., we vary the temperature T. And in the right plot we show two curves with slightly different transverse forces at zero temperature: $\sigma(T = 0, F_x^{\mathrm{L}}, F_y^{\mathrm{L}} = 0.00225 f_0)$ and $\sigma(T = 0, F_x^{\mathrm{L}}, F_y^{\mathrm{L}} = 0.00275 f_0)$, i.e., we vary the longitudinal driving force F_x^{L}.

In the left plot in Fig. 6 the constant transverse force $F_x^{\mathrm{L}} = 1 f_0$ results in a velocity of $v_x \approx 1$ simulation units, and the transverse force $F_y^{\mathrm{L}} = 0.00225 f_0$ is chosen to be slightly smaller than the critical transverse force at $T = 0$ for these simulations. The plot shows that for very small temperatures $\sigma \approx 0$. This means that an increase in the transverse force does not result in an increase in transverse motion. With increasing temperature σ shows a peak. Here, an increase in the transverse force results in a strong increase in the transverse velocity, and this is where the system starts quickly moving transversely. For a further increase in temperature, σ comes down to $\sigma \approx 1.2$, before it drops to 1.0 at the melting temperature T_m. The reason that $\sigma \approx 1.2$ for intermediate temperatures is that even after transverse depinning the moving system feels some transverse pinning up to transverse forces many times larger than the critical transverse force.[13] The remaining transverse pinning reduces with increasing transverse drive, F_y^{L}, and we find the transverse response, v_y, to be nonlinear in this regime: v_y increases stronger than linearly with F_y^{L}. Thus, $\sigma = (\mathrm{d}v_y/\mathrm{d}F_y^{\mathrm{L}})/R_x > 1$.

The right plot in Fig. 6 shows zero-temperature data for various longitudinal driving forces F_x^{L} and two different constant transverse forces $F_y^{\mathrm{L}} = 0.00225 f_0$ and $F_y^{\mathrm{L}} = 0.00275 f_0$. For small F_x^{L} the system does not move transversely and $\sigma = 0$. When F_x^{L} increases, it increases the velocity v_x of the system and thus reduces the critical transverse force (as shown in Fig. 4). Therefore, for sufficiently large F_x^{L} the system starts moving transversely and σ shows a peak which decays to 1.0 for larger F_x^{L}. The slow decay of σ is due to remaining transverse pinning above the transverse depinning force.[13] The magnitude of the constant transverse driving force F_y^{L} determines the position of the peak of σ, as the two curves in the right plot in Fig. 6 demonstrate. In experimental work the presence of a critical transverse force should manifest itself in σ changing as shown in Fig. 6.

IV. SUMMARY

We have investigated numerically the critical transverse force of two-dimensional vortex systems in the presence of a random pinning potential. We find a critical transverse force for both the MBG and the MTG, but not for turbulent plastic flow. The ratio of the critical transverse force to the static depinning force is of the order of 10%. For the MBG we find that the critical transverse force increases with increasing pinning strength up to a value at which the elastic motion changes to turbulent plastic flow and the critical transverse force goes rapidly to zero. The critical transverse force is inversely proportional to the longitudinal velocity and is compatible with theoretical predictions.[8]

We have performed simulations in which a hexagonal lattice is driven in low higher-order lattice directions. These simulations revealed that a MBG and a critical transverse force exist for the driving force in the [21] direction, but not for the [31] and higher-order directions, thus supporting the theory of Giamarchi and Le Doussal.[7] Our results suggest that in an experimental search for the critical transverse current low temperatures and small longitudinal driving forces (which, however, will have to be large enough to cause elastic motion) are most promising. We provide data that can be compared directly with experimental efforts to demonstrate a critical transverse force.

ACKNOWLEDGMENTS

We thank P. Le Doussal, A. R. Price, and S. Gordeev for helpful discussions. We acknowledge financial support from DAAD and EPSRC.

[1] S. Bhattacharya and M.J. Higgins, Phys. Rev. Lett. **70**, 2617 (1993); U. Yaron, P.L. Gammel, D.A. Huse, R.N. Kleiman, C.S. Oglesby, E. Bucher, B. Batlogg, D.J. Bishop, K. Mortensen, K. Clausen, C.A. Bolle, and F. De La Cruz, *ibid.* **73**, 2748 (1994); M.C. Hellerqvist, D. Ephorn, W.R. White, M.R. Beasley, and A. Kapitulnik, *ibid.* **76**, 4022 (1996); F. Pardo, F. De La Cruz, P.L. Gammel, C.S. Oglesby, E. Bucher, B. Batlogg, and D.J. Bishop, *ibid.* **78**, 4633 (1997).

[2] A.E. Koshelev and V.M. Vinokur, Phys. Rev. Lett. **73**, 3580 (1994).

[3] H.J. Jensen, A. Brass, and A.J. Berlinsky, Phys. Rev. Lett. **60**, 1676 (1988).
[4] K. Moon, R.T. Scalettar, and G.T. Zimányi, Phys. Rev. Lett. **77**, 2778 (1996).
[5] S. Ryu, M. Hellerqvist, S. Doniach, A. Kapitulnik, and D. Stroud, Phys. Rev. Lett. **77**, 5114 (1996).
[6] C.J. Olson, C. Reichhardt, and F. Nori, Phys. Rev. Lett. **81**, 3757 (1998).
[7] T. Giamarchi and P. Le Doussal, Phys. Rev. Lett. **76**, 3408 (1996).
[8] P. Le Doussal and T. Giamarchi, Phys. Rev. B **57**, 11 356 (1998).
[9] L. Balents, M.C. Marchetti, and L. Radzihovsky, Phys. Rev. B **57**, 7705 (1998).
[10] S. Scheidl and V.M. Vinokur, Phys. Rev. E **57**, 2574 (1998).
[11] F. Pardo, F. de la Cruz, P.L. Gammel, E. Bucher, and D.J. Bishop, Nature (London) **396**, 348 (1998); A.M. Troyanovski, J. Aarts, and P.H. Kes, *ibid.* **399**, 665 (1999).
[12] A.B. Kolton and D. Domínguez, Phys. Rev. Lett. **83**, 3061 (1999).
[13] C.J. Olson and C. Reichhardt, Phys. Rev. B **61**, R3811 (2000).
[14] C. Reichhardt and F. Nori, Phys. Rev. Lett. **82**, 414 (1999); V.I. Marconi and D. Domínguez, *ibid.* **82**, 4922 (1999).
[15] J.R. Clem, Phys. Rev. B **43**, 7837 (1991).
[16] H. Fangohr, A. Price, S. Cox, P.A.J. de Groot, G.J. Daniell, and K.S. Thomas, J. Comput. Phys. **162**, 372 (2000).
[17] H. Fangohr, S. J. Cox, and P. A. J. de Groot (unpublished).